J|A|C|S
ARTICLES
Published on Web 10/12/2004

Epitope Mapping and Competitive Binding of HSA Drug Site II Ligands by NMR Diffusion Measurements

Laura H. Lucas, Kristin E. Price, and Cynthia K. Larive*

Contribution from the Department of Chemistry, University of Kansas, Lawrence, Kansas 66045

Received April 8, 2004; E-mail: clarive@ku.edu

Abstract: It is important to characterize drug−albumin binding during drug discovery and lead optimization as strong binding may reduce bioavailability and/or increase the drug's in vivo half-life. Despite knowing about the location of human serum albumin (HSA) drug binding sites and the residues important for binding, less is understood about the binding dynamics between exogenous drugs and endogenous fatty acids. In contrast to highly specific antibody−antigen interactions, the conformational flexibility of albumin allows the protein to adopt multiple conformations of approximately equal energy in order to accommodate a variety of ligands. Nuclear magnetic resonance (NMR) diffusion measurements are a simple way to quantitatively describe ligand−protein interactions without prior knowledge of the number of binding sites or the binding stoichiometry. This method can also provide information about ligand orientation at the binding site due to buildup of exchange-transferred NOE (trNOE) on the diffusion time scale of the experiment. The results of NMR diffusion and NOE experiments reveal multiple binding interactions of HSA with dansylglycine, a drug site II probe, and caprylate, a medium-chain fatty acid that also has primary affinity for HSA's drug site II. Interligand NOE (ilNOE) detected in the diffusion analysis of a protein solution containing both ligands provides insight into the conformations adopted by these ligands while bound in common HSA binding pockets. The results demonstrate the ability of NMR diffusion experiments to identify ternary complex formation and show the potential of this method for characterizing other biologically important ternary structures, such as enzyme−cofactor−inhibitor complexes.

Introduction

It is important to characterize drug−albumin binding during drug discovery and lead optimization as strong binding may reduce bioavailability and/or increase the drug's in vivo half-life.[1] Sudlow's pioneering work in the mid-1970s revealed two major drug binding sites in albumin by equilibrium dialysis and fluorescence competition experiments.[2] Crystal structures of human serum albumin (HSA) have shown that both binding pockets contain cationic residues near the surface and have hydrophobic interiors.[3,4] In recent years, albumin has been cocrystallized with a variety of ligands including fatty acids,[5−8] triiodobenzoic acid,[4] the anticoagulant warfarin,[9,10] and the general anesthetics propofol and halothane.[10] Collectively the results show that although the basic chemistry involved in ligand binding at HSA drug sites I and II is similar, the orientation and specificity of individual ligands depend largely on their structures.[1,3]

Despite knowledge of the location of HSA drug binding sites and the residues important for binding specific ligands, less is understood about the binding dynamics of exogenous drugs and endogenous fatty acids. This area merits scientific consideration given that endogenous ligands can reduce the drug−albumin interaction, as reported for patients with chronic renal failure.[11] In contrast to highly specific antibody−antigen interactions, the conformational flexibility of albumin allows the protein to adopt multiple conformations of approximately equal energy in order to accommodate a variety of ligands.[12,13] The research described herein reveals the binding epitopes of dansylglycine, an albumin drug site II probe and caprylate, a medium-chain fatty acid that also has primary affinity for HSA drug site II, on the basis of NMR diffusion and nuclear Overhauser effect (NOE) experiments (Chart 1).

Experimental Methods

Sample Preparation. Human serum albumin (essentially fatty acid and globulin free), dansylglycine, and caprylic acid (sodium salt, 99+% pure) were purchased from Sigma Chemical Co. (St. Louis, MO). The

(1) Kragh-Hansen, U.; Chuang, V. T. G.; Otagiri, M. *Biol. Pharm. Bull.* **2002**, *25*, 695−704.
(2) Sudlow, G.; Birkett, D. J.; Wade, D. N. *Mol. Pharmacol.* **1975**, *11*, 824−832.
(3) Sugio, S.; Kashima, A.; Mochizuki, S.; Noda, M.; Kobayashi, K. *Protein Eng.* **1999**, *12*, 439−446.
(4) He, X. M.; Carter, D. C. *Nature* **1992**, *358*, 209−215.
(5) Bhattacharya, A. A.; Grüne, T.; Curry, S. *J. Mol. Biol.* **2000**, *303*, 721−732.
(6) Curry, S.; Brick, P.; Franks, N. P. *Biochim. Biophys. Acta* **1999**, *1441*, 131−140.
(7) Curry, S.; Mandelkow, H.; Brick, P.; Franks, N. *Nat. Struct. Biol.* **1998**, *5*, 827−835.
(8) Petitpas, I.; Grüne, T.; Bhattacharya, A. A.; Curry, S. *J. Mol. Biol.* **2001**, *314*, 955−960.
(9) Petitpas, I.; Bhattacharya, A. A.; Twine, S.; East, M.; Curry, S. *J. Biol. Chem.* **2001**, *276*, 22804−22809.
(10) Bhattacharya, A. A.; Curry, S.; Franks, N. P. *J. Biol. Chem.* **2000**, *275*, 38731−38738.
(11) Robertz, G.-M.; Dengler, H. J. *Klin. Wochenschr.* **1983**, *61*, 649−653.
(12) Karush, F. *J. Am. Chem. Soc.* **1950**, *72*, 2705−2713.
(13) Karush, F. *J. Am. Chem. Soc.* **1950**, *72*, 2714−2718.

10.1021/ja0479538 CCC: $27.50

Chart 1. HSA Drug Site II Ligands[a]

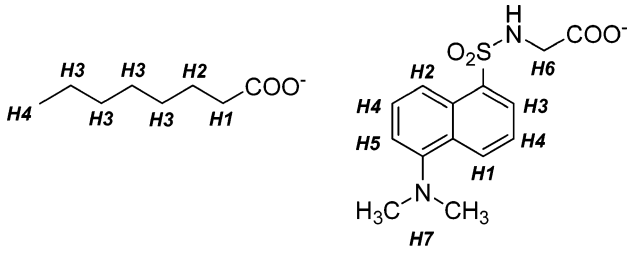

Caprylate (CAP) Dansylglycine (DG)

[a] Italicized labels correspond to the ligand proton designations indicated in Figure 1 and throughout the text.

ligand structures are shown in Chart 1. All solutions were prepared in 25 mM sodium phosphate dissolved in D_2O, pD 7.80 ± 0.01. The buffer salts (Fisher Scientific, Fair Lawn, NJ) were doubly lyophilized from D_2O to exchange protium for deuterium. All D_2O used was 99.9% atom D and purchased from Cambridge Isotope Laboratories, Inc. (CIL, Cambridge, MA). Stock solutions were prepared at the following concentrations: 1.00 mM HSA (based on a molecular mass of 66 478 Da), 50.0 mM caprylate, and 8.00 mM dansylglycine. All solutions analyzed were prepared by diluting from these stock solutions with the buffer described above. Because of caprylate's higher aqueous solubility relative to dansylglycine, the 25:1 solution of caprylate:HSA (CAP:HSA) contained 12.5 mM caprylate and 500 μM HSA. The concentrations of caprylate in both the stock and diluted solutions were well below the reported critical micelle concentration of 0.38 M.[14,15] All other solutions, including the 25:25:1 dansylglycine:caprylate:HSA (DG:CAP:HSA) solution contained 100 μM protein. The solutions were stored at 4 °C until analyzed.

NMR Spectroscopy. The samples were analyzed by ^{1}H NMR at 25.0 ± 0.1 °C on a Varian INOVA 600 MHz spectrometer (Varian Instruments, Inc., Palo Alto, CA) using a 5 mm triple-axis gradient probe. Shigemi NMR tubes (Shigemi Co., Ltd., Allison Park, PA) susceptibility matched for D_2O were used to restrict the volume of each sample to the active volume of the NMR probe. The *b*ipolar *p*ulse *p*air *st*imulated *e*cho (BPPSTE) pulse sequence[16−19] was used for all diffusion measurements. WET (*w*ater *e*liminated by *t*ransverse gradients) was incorporated into the relaxation delay to suppress the HOD resonance.[20] To selectively excite solvent protons, 18 ms sinc pulses were used followed by a 2.0 ms gradient pulse and 2.0 ms recovery time. This sequence was repeated four times followed by a final 6.0 ms delay before the first 90° pulse of the BPPSTE experiment.

Diffusion and NOE Experiments. Individual ligand and protein diffusion coefficients were determined by performing BPPSTE experiments on the following solutions: 12.5 mM caprylate, 2.5 mM dansylglycine, and 500 μM HSA using gradient pulses (δ/2) of 1.5 ms (dansylglycine) or 2.0 ms (caprylate, HSA) followed by a gradient recovery time (τ) of 50 μs. The effective diffusion delay time (T) was 50 ms. The free ligand diffusion coefficients were corrected for the viscosity of the protein solutions (Supporting Information). The errors in the corrected diffusion coefficients include the errors in the viscosity measurements. For all ligand−protein solutions, separate experiments were performed at T of 50, 200, 400, 600, and 800 ms using a gradient pulse of 1.5 ms followed by a gradient recovery time of 50 μs. The gradient amplitudes and number of increments acquired varied according to T. Identical experiments were acquired for each T value for the 100 and 500 μM HSA solutions alone for spectral subtraction to remove the spectral background arising from the protein resonances.[21] In addition, NOESY spectra were acquired at a mixing time (t_m) of 400 ms for solutions of 1:1 DG:CAP (2.5 mM each) and 25:25:1 DG:CAP:HSA.

Analysis of Diffusion Data. In all cases, spectra were phased and baseline-corrected prior to subtraction to remove the protein background and minor adjustments were made in the final subtracted spectra when necessary. The spectra were referenced to the residual HOD peak (4.78 ppm) detected in a ^{1}H experiment acquired without solvent suppression. Resonance integrals were measured in the spectra of the free dansylglycine, free caprylate, and HSA solutions. Ligand peak intensities were measured in the subtracted spectra. When dansylglycine or caprylate peaks were not visible above the noise, those spectra were not included in the calculation of dansylglycine or caprylate diffusion coefficients. These integrals or intensities were fit to eq 2 by a nonlinear least-squares algorithm using Scientist (MicroMath, Inc., Salt Lake City, UT). The errors reported for diffusion coefficients of individual ligand functional groups are the fitting errors calculated in Scientist. Data were also plotted according to the linear version of eq 2 using Origin 7.0 (OriginLab Corp., Northampton, MA). The best fits of the diffusion data to a second-order polynomial were used to obtain κ values (coefficient of the squared term), with fitting errors reported. A factor of $(2\pi)^2$ was inadvertently omitted from the denominator of the y-axis in the graphs shown in Figures 2, 3, and S1 but is included in the analysis used to obtain the reported absolute κ values (Figure 4 and Table S1). Normalized κ values (Figure 4) may vary by ±1%.

Results

NMR diffusion measurements are a simple way to quantitatively describe ligand−protein interactions without prior knowledge of the number of binding sites or the binding stoichiometry.[22] When a small molecule interacts with a much larger protein, it assumes the translational diffusivity of the protein, resulting in a significant change in its diffusion coefficient. In the limit of fast chemical exchange on the time scale of the diffusion measurement, a single set of ligand resonances is observed in the spectrum that represents the average behavior of the ligand in the free and bound states.[23] The measured ligand diffusion coefficient, D_o, is the weighted average diffusion coefficient for the ligand in the free (D_f) and bound (D_b) states.

$$D_o = (D_f f_f) + (D_b f_b) \quad (1)$$

In eq 1, f_f and f_b are the fractions of free and bound ligand, respectively. Equation 1 is useful for calculating binding constants, if the binding occurs with defined stoichiometry,[21] for identifying the presence of multiple binding sites, and revealing the relative binding capacities of several ligands.[24]

Diffusion measurements are possible using pulse sequences incorporating pulsed-field gradients.[17] Signal decay as a function of gradient amplitude (g) is monitored, with the results fit to eq 2 to determine the diffusion coefficient (D):

(14) Ekwall, P. In *Chemistry, Physics and Application of Surface Active Substances, Proceedings of the International Congress on Surface Active Substances, 4th*; Overbeek, J. T. G., Ed.; Gordon and Breach: Stockholm, Sweden, 1964; Vol. 2, pp 651−658.
(15) Geankoplis, C. J.; Hu, M. C. *Ind. Eng. Chem. Fundam.* **1982**, *21*, 135−141.
(16) Otto, W. H.; Larive, C. K. *J. Magn. Reson.* **2001**, *153*, 1−4.
(17) Pelta, M. D.; Barjat, H.; Morris, G. A.; Davis, A. L.; Hammond, S. J. *Magn. Reson. Chem.* **1998**, *36*, 706−714.
(18) Tanner, J. E. *J. Chem. Phys.* **1970**, *52*, 2523−2526.
(19) Wu, D.; Chen, A.; Johnson, J., C. S. *J. Magn. Reson., Ser. A* **1995**, *115*, 260−264.
(20) Smallcombe, S. H.; Patt, S. L.; Keifer, P. A. *J. Magn. Reson., Ser. A* **1995**, *117*, 295−303.
(21) Derrick, T. S.; McCord, E. F.; Larive, C. K. *J. Magn. Reson.* **2002**, *155*, 217−225.
(22) Lucas, L. H.; Larive, C. K. *Concepts Magn. Reson., Part A* **2004**, *20A*, 24−41.
(23) Johnson, C. S., Jr. *J. Magn. Reson., Ser. A* **1993**, *102*, 214−218.
(24) Liu, M.; Nicholson, J. K.; Lindon, J. C. *Anal. Commun.* **1997**, *34*, 225−228.

$$I = I_o \exp[-D(\gamma\delta g)^2(\Delta - \delta/3 - \tau/2)] \quad (2)$$

In eq 2, I_o is the signal intensity (or integral) in the absence of an applied magnetic field gradient, γ is the gyromagnetic ratio of the nucleus analyzed, δ is the duration of the gradient pulse pair, Δ is the total experimental diffusion time, and τ is a short gradient recovery delay. By taking the natural log of both sides of eq 2, a linear equation results, and D is determined from the slope.

Diffusion NMR measurements have been widely applied to problems of pharmaceutical relevance including drug screening[25] and characterization of enzyme−inhibitor binding.[26,27] More recently, this technique has been developed as a method for ligand epitope mapping.[28−31] Information about the ligand binding epitope is obtained by conducting the diffusion experiments at relatively long diffusion delay times (∼500−1000 ms). Under these conditions, detectable transferred NOE (trNOE) builds up on the time scale of the measurement and disrupts the expected signal decay due to diffusion. The resulting diffusion data sets are curved rather than linear. Since trNOE is most pronounced for ligand functional groups in close proximity to the protein at the binding site,[32−35] quantifying the curvature provides a direct way to generate the ligand epitope map.

Figure 1 shows the ^{1}H BPPSTE spectra acquired at the lowest gradient amplitude and a short effective diffusion delay time ($T = 50$ ms) for several ligand:HSA mixtures using the method of spectral subtraction[21] to eliminate the HSA background signal. T is approximately equal to Δ but accounts only for the time the magnetization is stored along the $\pm z'$ axis, where both trNOE and diffusion affect the detected resonance intensities.[22] A single set of resonances is observed for both caprylate, a medium chain fatty acid, and dansylglycine (Chart 1), a drug analogue, in HSA solutions. The chemical shifts of the ligand resonances represent the weighted average of the free and bound ligand. Splitting of individual resonances due to ^{1}H−^{1}H J coupling cannot be resolved, and the ligand resonances are observed as broad singlets. NMR resonance line widths are related inversely to the nuclear T_2 relaxation times, which are generally shorter for large molecules, such as proteins, than for small ligands. Therefore, the broadened ligand resonances observed in Figure 1 indicate that each ligand binds strongly to HSA, assuming the motional properties of the protein upon binding. Additional line broadening may also arise from intermediate chemical exchange on the NMR chemical shift time scale.[22] However, when titrating DG or CAP into protein solutions containing the other ligand, no changes in ligand chemical shifts were observed.

Competitive interactions are certainly influential in the DG:CAP:HSA system, since both ligands have similar affinities for a common primary binding site. Qualitative examination of Figure 1 shows decreased line widths when both ligands are present in the albumin solution, indicating competitive binding. Although a direct comparison cannot be made between spectra 1A and 1D for caprylate due to the different gradient durations used, the effect of the competing ligand is especially noticeable for caprylate resonances.

Competitive interactions are also suggested by the diffusion coefficients obtained for dansylglycine and caprylate in these solutions. The diffusion data measured for the free ligands and the ligand:protein mixtures are plotted in Figure 2 according to the linear version of eq 2. For both ligands only the data for the $-CH_2$ group adjacent to the carboxylate group is displayed: DG *H6* in Figure 2A and CAP *H1* in Figure 2B (refer to Chart 1 for structures). The carboxylate group of both ligands is thought to have an important electrostatic interaction with HSA, since anions but not cations were observed to bind to HSA drug site II[36] and a positively charged residue is positioned near the entrance of the binding pocket.[3] Because the acidic protons are not detectable by NMR spectroscopy, the adjacent methylene groups are a good choice for monitoring the interactions of these ligands with HSA. The slope of the 2.5 mM DG data in Figure 2A is greater than the slopes obtained from the analysis of solutions containing DG and protein, showing that the rate of dansylglycine diffusion decreases due to HSA binding. The viscosity-corrected diffusion coefficient for dansylglycine, $(4.98 \pm 0.06) \times 10^{-10}$ m^2/s in buffer solution alone, decreases to $(4.53 \pm 0.03) \times 10^{-10}$ m^2/s when the protein is introduced. The viscosity-corrected diffusion coefficient for caprylate, $(5.88 \pm 0.01) \times 10^{-10}$ m^2/s in buffer solution alone, decreases to $(4.12 \pm 0.04) \times 10^{-10}$ m^2/s when the protein is introduced. Both decreases are significant within the experimental errors and indicate that each ligand binds to HSA. When a small amount of caprylate is added, the diffusion coefficient for DG *H6* is $(4.44 \pm 0.09) \times 10^{-10}$ m^2/s, which agrees within error with the DG *H6* diffusion coefficient obtained for the 25:1 DG:HSA solution. However as discussed below, for the 25:1:1 solution the effects of chemical exchange obscure direct interpretation of this value. Upon addition of more caprylate, the dansylglycine diffusion coefficient increases to $(4.71 \pm 0.06) \times 10^{-10}$ m^2/s, suggesting that the caprylate competitively displaces the dansylglycine. The caprylate diffusion coefficient changes in a more dramatic fashion when the dansylglycine is added, increasing by 38% relative to its diffusion coefficient in the presence of protein only. The increase in both ligand diffusion coefficients (and the decrease in resonance line widths, Figure 1) when the other ligand is added suggests competition for common albumin binding sites.

The biexponential behavior of the 25:1:1 DG:CAP:HSA data measured for $T = 50$ ms in Figure 2A suggests that the competitive binding of a small amount of caprylate has altered the binding kinetics and the exchange between free and bound DG is no longer fast on the NMR diffusion time scale, which is defined by T.[23,37] Curvature in diffusion plots arising from chemical exchange is not specific to certain ligand functional

(25) Chen, A.; Shapiro, M. J. *Anal. Chem.* **1999**, *71*, 669A−675A.
(26) Derrick, T. S.; Lucas, L. H.; Dimicoli, J.-L.; Larive, C. K. *Magn. Reson. Chem.* **2002**, *40*, S98−S105.
(27) Atkinson, C. E.; Aliev, A. E.; Motherwell, W. B. *Chem. Eur. J.* **2003**, *9*, 1714−1722.
(28) Chen, A.; Shapiro, M. J. *J. Am. Chem. Soc.* **1999**, *121*, 5338−5339.
(29) Lucas, L. H.; Yan, J.; Larive, C. K.; Zartler, E. R.; Shapiro, M. J. *Anal. Chem.* **2003**, *75*, 627−634.
(30) Yan, J.; Kline, A. D.; Mo, H.; Shapiro, M. J.; Zartler, E. R. *J. Magn. Reson.* **2003**, *163*, 270−276.
(31) Yan, J.; Kline, A. D.; Mo, H.; Zartler, E. R.; Shapiro, M. J. *J. Am. Chem. Soc.* **2002**, *124*, 9984−9985.
(32) Campbell, A. P.; Sykes, B. D. *J. Magn. Reson.* **1991**, *93*, 77−92.
(33) Clore, G. M.; Gronenborn, A. M. *J. Magn. Reson.* **1983**, *53*, 423−442.
(34) Neuhaus, D.; Williamson, M. P. *The Nuclear Overhauser Effect in Structural and Conformational Analysis*; 2nd ed.; Wiley-VCH: New York, 2000.
(35) Post, C. B. *Curr. Opin. Struct. Biol.* **2003**, *13*, 581−588.
(36) Wanwimolruk, S.; Birkett, D. J.; Brooks, P. M. *Mol. Pharmacol.* **1983**, *24*, 458−463.
(37) Cabrita, E. J.; Berger, S.; Brauer, P.; Karger, J. *J. Magn. Reson.* **2002**, *157*, 124−131.

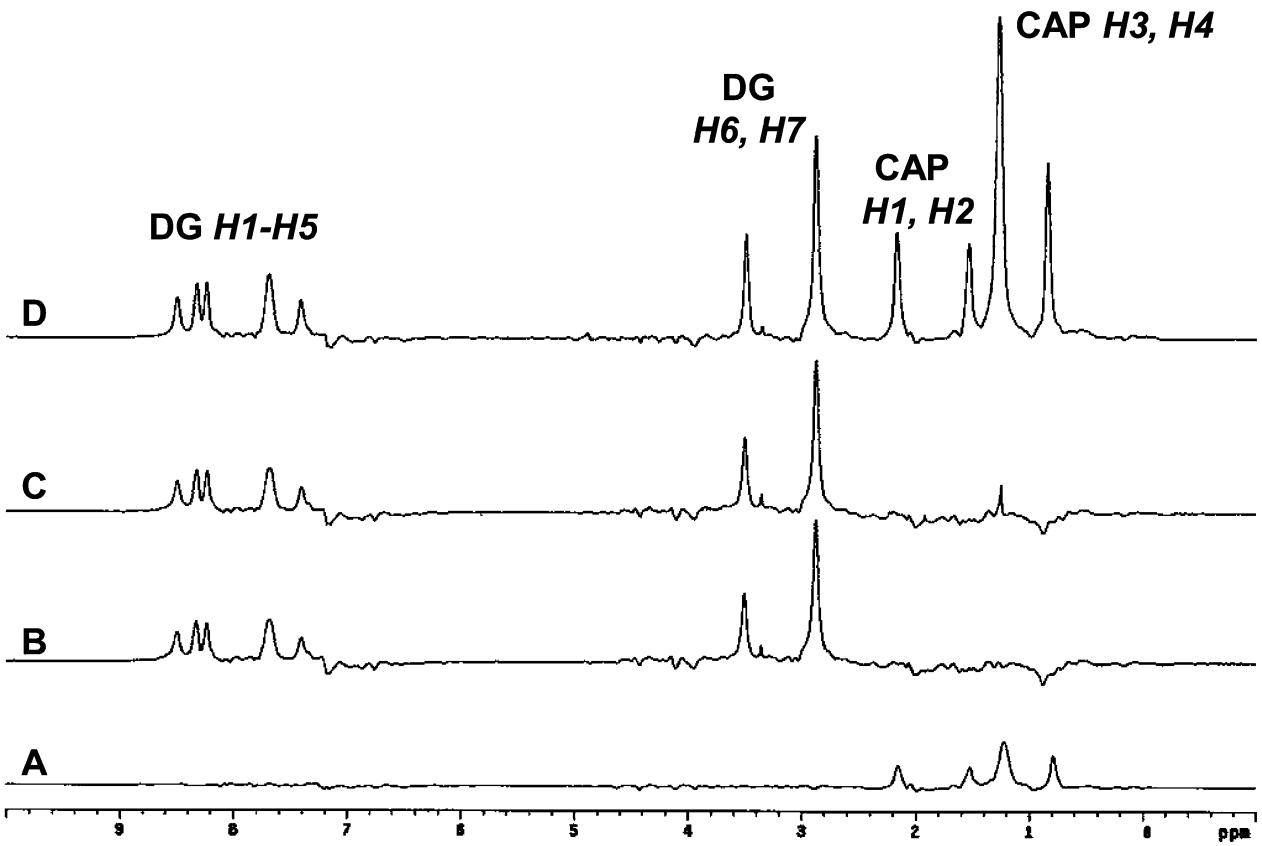

Figure 1. ^{1}H BPPSTE spectra for dansylglycine (DG) and caprylate (CAP) in various mixtures with HSA. The protein spectral background has been subtracted. All spectra were acquired with $g = 227$ G/m, $\tau = 50$ μs, and $T = 50$ ms. (A) 25:1 CAP:HSA, (B) 25:1 DG:HSA, (C) 25:1:1 DG:CAP:HSA, and (D) 25:25:1 DG:CAP:HSA. The proton designations correspond to the structures shown in Chart 1 and are assigned from left to right across the spectra. The gradient amplitude was 2.0 ms in A and 1.5 ms in B−D. The small peaks observed in B and C between 0 and 2.5 ppm are spectral subtraction artifacts.

groups, and the observed deviation from linearity is similar for each dansylglycine proton (Figure S1, Supporting Information). However, curvature arising from the trNOE should be different for individual ligand functional groups, based on specific ligand−protein interactions.[29,31] As shown in Figure 2A, curvature at low T is not observed when the solution contains equivalent concentrations of DG and caprylate, suggesting that the population of bound dansylglycine decreases resulting in fast exchange on the time scale of the diffusion measurement.[37]

Figure 3 shows the diffusion data for the DG *H6* and CAP *H1* methylene groups in the different protein mixtures at $T =$ 600 ms. Clearly, the most curved plots are observed when an excess of both ligands is used. The curvature is quantitatively described by the coefficient of the squared term (κ) obtained by fitting a second-order polynomial equation to the diffusion data.[30,31] Higher κ values indicate greater curvature and hence closer contacts with the protein. Epitope maps are generated by normalizing κ values measured for each ligand proton resonance to the highest κ value observed for the ligand (Figure 4). Analysis of the curvature provides insight into the orientations of HSA-bound dansylglycine and caprylate.

Traditionally, trNOE is detected in a two-dimensional (2D) NOESY experiment, where NOE builds up during the mixing time, t_m.[33,34] The NOE mixing time is analogous to the effective diffusion delay time, T, because in both instances the magnetization is aligned along the $\pm z'$ axis. In this orientation dipolar relaxation occurs, which is the origin of the NOE.[33,34] For solutions where ligand−protein interactions occur, the sign of the ligand NOE cross-peaks will change due to binding to the protein. This results from an increase in the rotational correlation time, τ_c, as the ligand binds and assumes the slow tumbling properties of the protein in solution. In our experiments, positive intramolecular cross-peaks were observed for the ligand mixture in the absence of the protein (Figure S2, Supporting Information) revealing no inherent interaction of the two small molecules. However, as shown in Figure 5, negative intraligand cross-peaks (circled) are observed for each ligand due to trNOE, indicating both binding to the protein and intraligand interactions at the binding site. Negative *i*nter*l*igand *NOE* (ilNOE) cross-peaks (boxed) are observed between dansylglycine and caprylate, revealing the simultaneous binding of both ligands to HSA. The ilNOE phenomenon is analogous to trNOE, except the cross-peaks are detected between the two ligands since they are exchanging in adjacent protein binding sites. This allows simultaneous binding of multiple ligands to be detected, permitting characterization of ternary structures such as albumin−drug−fatty acid or enzyme−cofactor−inhibitor complexes.[38−41]

(38) London, R. E. *J. Magn. Reson.* **1999**, *141*, 301−311.
(39) Li, D.; DeRose, E. F.; London, R. E. *J. Biomol. NMR* **1999**, *15*, 71−76.
(40) Li, D.; Levy, L. A.; Gabel, S. A.; Lebetkin, M. S.; DeRose, E. F.; Wall, M. J.; Howell, E. E.; London, R. E. *Biochemistry* **2001**, *40*, 4242−4252.
(41) Li, D.; London, R. E. *Biotechnol. Lett.* **2002**, *24*, 623−629.

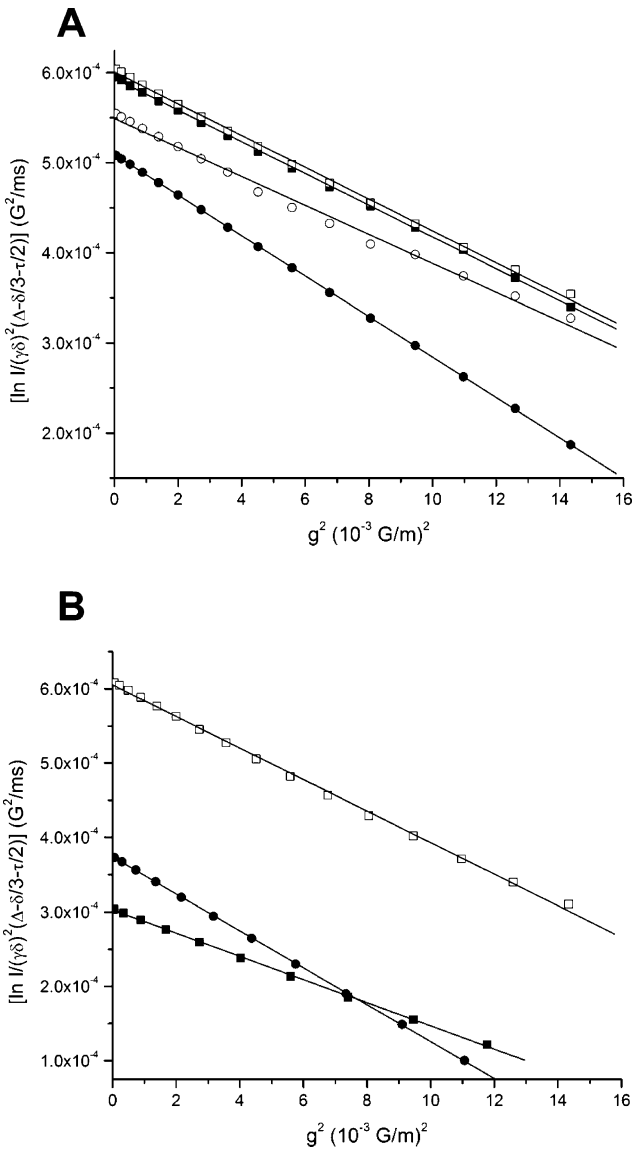

Figure 2. Diffusion data at $T = 50$ ms for DG *H6* (A) and CAP *H1* (B) in the various solutions studied. The data are plotted according to the linear version of eq 2 and displayed with the best linear fits. In A, the DG *H6* diffusion coefficients are as follows: $(4.98 \pm 0.06) \times 10^{-10}$ m^2/s (2.5 mM DG, ●), $(4.53 \pm 0.03) \times 10^{-10}$ m^2/s (25:1 DG:HSA, ■), $(4.44 \pm 0.09) \times 10^{-10}$ m^2/s (25:1:1 DG:CAP:HSA, ○), and $(4.71 \pm 0.06) \times 10^{-10}$ m^2/s (25:25:1 DG:CAP:HSA, □). In B the CAP *H1* diffusion coefficients are as follows: $(5.88 \pm 0.01) \times 10^{-10}$ m^2/s (12.5 mM CAP, ●), $(4.12 \pm 0.04) \times 10^{-10}$ m^2/s (25:1 DG:CAP:HSA, ■), and $(5.69 \pm 0.05) \times 10^{-10}$ m^2/s (25:25:1 DG:CAP:HSA, □).

Discussion

Human serum albumin is known to bind a variety of drugs and endogenous ligands, facilitating their transport throughout the circulatory system.[1,42−44] Albumin drug site II contains a hydrophobic pocket with the cationic side chain of Arg410 pointed toward the entrance of the binding cleft.[3,36] Dansylglycine, a fluorescent probe molecule used in drug competition studies, and caprylate, a highly soluble, medium-chain fatty acid,

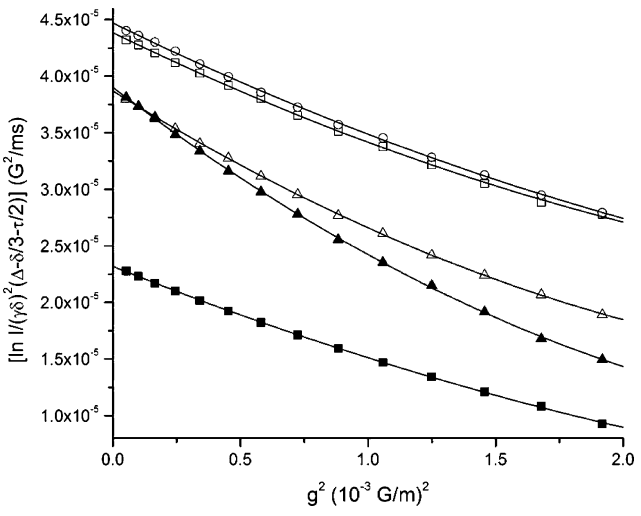

Figure 3. Diffusion data for DG *H6* and CAP *H1* as a function of solution composition. The open symbols represent dansylglycine diffusion and the closed symbols caprylate diffusion at $T = 600$ ms. The data are plotted according to the linear version of eq 2 and displayed with second-order polynomial fits. The intensities for the ligands in the 25:25:1 solution were measured at a lower vertical scale in the subtracted spectra so that differences in the individual data sets could be easily visualized on the *y*-axis scale displayed. The DG *H6* diffusion coefficients are as follows: $(2.32 \pm 0.05) \times 10^{-10}$ m^2/s (25:1 DG:HSA, □), $(2.38 \pm 0.05) \times 10^{-10}$ m^2/s (25:1:1 DG:CAP:HSA, ○), and $(2.94 \pm 0.08) \times 10^{-10}$ m^2/s (25:25:1 DG:CAP:HSA, △). The CAP *H1* diffusion coefficients are as follows: $(2.03 \pm 0.04) \times 10^{-10}$ m^2/s (25:1 CAP:HSA, ■) and $(3.69 \pm 0.10) \times 10^{-10}$ m^2/s (25:25:1 DG:CAP:HSA, ▲).

both bind strongly to site II with similar affinities ($K_d \approx 2$ μM).[45−48] Although the structures of these two molecules seem very different, both are relatively hydrophobic with one anionic end, the structural motif exhibited by drug site II ligands.[36,49]

Many of the results published thus far regarding HSA−ligand interactions have come from crystallographic data derived from the solid state, or from in situ competitive binding assays that require probe molecules containing radioactive or fluorescent labels, or the appropriate UV−visible absorption properties to detect and quantify binding. Nuclear magnetic resonance (NMR) spectroscopy is a valuable technique for studying dynamic ligand−protein interactions because structural information is gained noninvasively for the ligand−protein solution, without requiring a separation.[50] A major advantage of NMR is that nearly all molecules contain NMR-active nuclei, eliminating the need for fluorescent or radioactive labels. The nature of the NMR signal allows information about specific functional groups to be obtained for multiple molecules, provided that at least one NMR resonance of each molecule is well-resolved in the spectrum. This enables simultaneous analysis of multiple ligands interacting with HSA, allowing the investigation of the impact one ligand may have on the binding of another.

In addition to quantitatively describing binding affinity, NMR diffusion measurements can also provide information about ligand orientation at the binding site.[28−31] Traditionally, trNOE is detected as intraligand cross-peaks of negative intensity in

(42) Kragh-Hansen, U. *Dan. Med. Bull.* **1990**, *37*, 57−84.
(43) McMenamy, R. H. In *Albumin Structure, Function and Uses*; Rosenoer, V. M., Oratz, M., Rothschild, M. A., Eds.; Pergamon Press: Elmsford, NY, 1977; pp 143−158.
(44) Sellers, E. M.; Koch-Weser, J. In *Albumin Structure, Function and Uses*; Rosenoer, V. M., Oratz, M., Rothschild, M. A., Eds.; Pergamon Press: Elmsford, NY, 1977; pp 159−182.
(45) Muller, N.; Lapicque, F.; Drelon, F.; Netter, P. *J. Pharm. Pharmacol.* **1994**, *46*, 300−304.
(46) Kragh-Hansen, U. *Biochem. J.* **1991**, *273*, 641−644.
(47) Koh, S.-W. M.; Means, G. E. *Arch. Biochem. Biophys.* **1979**, *192*, 73−79.
(48) Kasai, S.; Horie, T.; Mizuma, T.; Awazu, S. *J. Pharm. Sci.* **1987**, *76*, 387−392.
(49) Sudlow, G.; Birkett, D. J.; Wade, D. N. *Mol. Pharmacol.* **1976**, *12*, 1052−1061.
(50) Meyer, B.; Peters, T. *Angew. Chem., Int. Ed.* **2003**, *42*, 864−890.

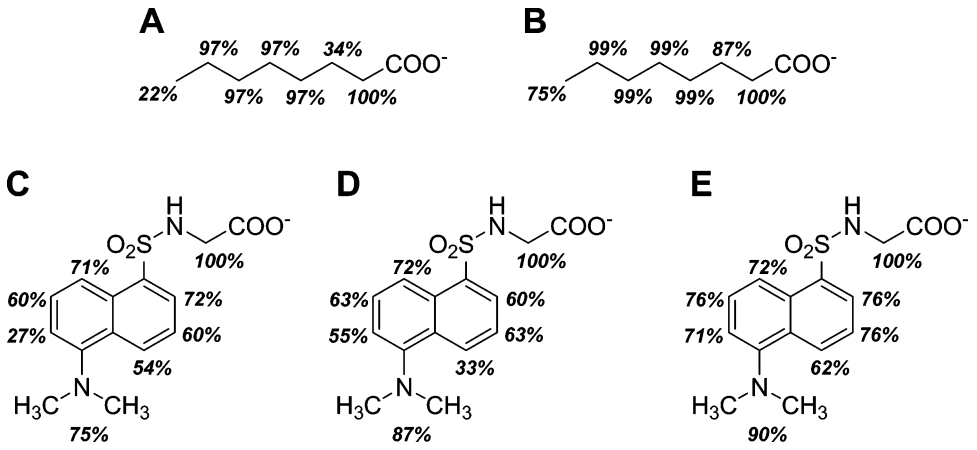

Figure 4. Dansylglycine and caprylate epitope maps derived from the polynomial analysis of diffusion data at $T = 600$ ms. The percentages represent normalized κ values obtained from the polynomial fits and are used to quantitatively describe which ligand functional groups are in closest contact with the protein. (A) Caprylate epitope in the 25:1 CAP:HSA solution, (B) caprylate epitope in the 25:25:1 DG:CAP:HSA solution, (C) dansylglycine epitope in the 25:1 DG:HSA solution, (D) dansylglycine epitope in the 25:1:1 DG:CAP:HSA solution, and (E) dansylglycine epitope in the 25:25:1 DG:CAP:HSA solution. The maximum κ values for each ligand (all $\times 10^{-17}$ m^4 s^{-2}) are as follows: (A) 2.44, (B) 6.18, (C) 3.32, (D) 3.04, and (E) 5.03. The individual κ values for the CAP *H3* methylene groups could not be distinguished due to spectral degeneracy.

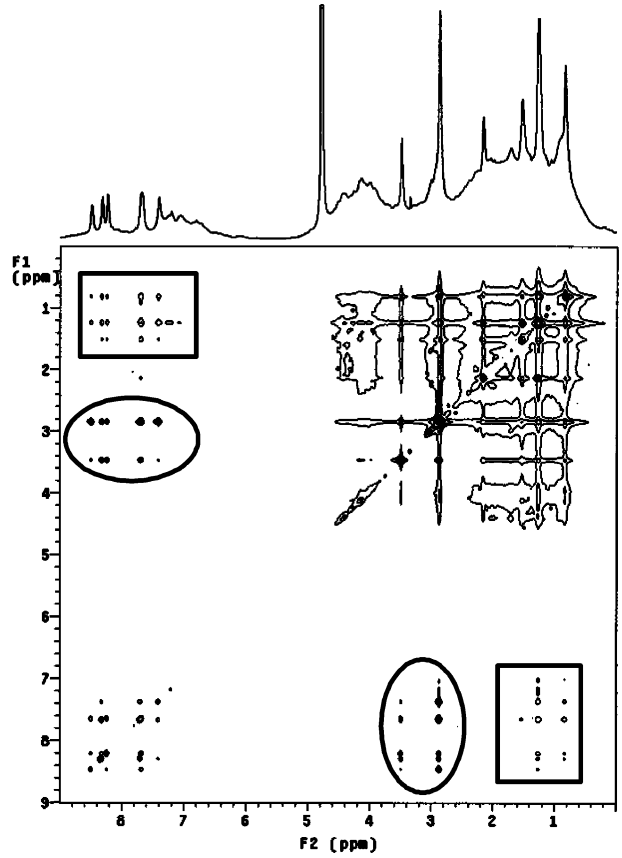

Figure 5. NOESY spectrum acquired at $t_m = 400$ ms for the 25:25:1 DG:CAP:HSA solution. All cross-peaks are the same phase as the diagonal. Intraligand cross-peaks (circled) arise from trNOE and indicate binding, while ilNOE cross-peaks (boxed) between the two ligands indicate that they are adjacent to one another in common binding pockets. The 1D ^{1}H spectrum acquired without water suppression is displayed above the 2D plot. For display purposes, the spectral noise in the 2D data arising from the solvent has been omitted. NOE cross-peaks between CAP H1 and DG protons are visibile if the spectrum is displayed at a higher vertical scale.

two-dimensional (2D) NOESY spectra. The detectable NOE develops in the NOESY experiment when the magnetization is aligned along the $\pm z'$ axis, during the experimental mixing time. The buildup of NOE cross-peak intensity can be measured for NOESY spectra acquired at different mixing times to determine bound ligand conformation.[51−54]

The NMR diffusion experiment is also useful for obtaining details about the ligand binding epitope. Transferred NOE that builds up during T disrupts the measured signal decay due to diffusion resulting in curved data plotted according to the linearized version of eq 2.[28−31] Epitope maps are generated by analyzing the curvature of data acquired from a single diffusion experiment rather than a series of measurements performed as a function of time. While detecting trNOE by diffusion NMR has proven useful for epitope mapping of single ligands interacting with HSA, ligand binding in the presence of competing endogenous ligands such as fatty acids has yet to be investigated with this method.

Optimizing the Diffusion Experiment for Epitope Mapping: The Influence of T, trNOE, Spin Diffusion, and T_1 Relaxation. With the exception of the 25:1:1 DG:CAP:HSA data (Figure 2A), the diffusion results shown in Figure 2 are fit well by the linear version of eq 2. The lack of curvature for data measured with a short effective diffusion time is in agreement with the minimal trNOE typically observed at low mixing times and indicates the ligands are in fast chemical exchange on the diffusion time scale. The strikingly different diffusion coefficients, i.e., slopes, measured for free caprylate and caprylate in the presence of HSA is illustrated by the intersecting lines in Figure 2B. Competitive binding is suggested by the sharpening of ligand resonances and the diffusion coefficients extracted from the experimental data acquired with a short effective diffusion time represented in Figures 1 and 2, respectively. Under these experimental conditions, diffusion is a molecular property. Therefore, the analysis of the DG *H6* and CAP *H1* diffusion coefficients reflects the diffusion properties of the dansylglycine and caprylate molecules, respectively, as illustrated in Figure 2.[29]

The greater changes in the caprylate diffusion coefficient relative to that of dansylglycine suggests that the number of

(51) Weimar, T.; Stoffer, B.; Svensson, B.; Pinto, B. M. *Biochemistry* **2000**, *39*, 300−306.
(52) Ni, F. *Prog. Nucl. Magn. Reson. Spectrosc.* **1994**, *26*, 517−606.
(53) Meyer, B.; Weimar, T.; Peters, T. *Eur. J. Biochem.* **1997**, *246*, 705−709.
(54) Mayer, M.; Meyer, B. *J. Med. Chem.* **2000**, *43*, 2093−2099.

ligands bound per molecule of protein is greater for caprylate than dansylglycine, since the ligands have similar reported binding constants at drug site II.[45−48] At ligand:protein concentration ratios between 5:1 and 19:1, dansylglycine can bind at a secondary albumin site with a dissociation constant of 20 μM.[2] Caprylate binds to approximately 10 additional albumin sites with weaker affinities.[5,55] Therefore at a 25-fold excess of each ligand as used in these studies, it is likely that both ligands bind at multiple sites on albumin and the changes in ligand diffusion coefficients reflect the number of molecules bound as well as the affinities of those additional binding sites.

At longer T values, ligand exchange between the free and bound states becomes fast on the diffusion time scale and curvature due to chemical exchange was not observed for any of the solutions studied. Transferred NOE builds up during T, and the free ligand magnetization is preferentially attenuated by diffusion relative to the magnetization of ligands that bind to the protein during this time. This enables a more selective detection of the magnetization of binding ligands and therefore enhances the specificity of the epitopes generated from the diffusion data.

In NMR diffusion measurements made at high T values, there will be significant losses in resonance intensity due to T_1 relaxation. T_1 losses can reduce the ligand signal-to-noise ratio (S/N), making the diffusion data less precise. However, as long as the T_1 relaxation times for individual ligand protons are not largely different, information about the binding epitope should not be lost due to T_1 relaxation. This is an advantage over other eptiope mapping methods such as trNOESY, for which T_1 losses may affect the epitopes determined from NOE build-up curves.[51,56] The ligand T_1 relaxation times for DG and CAP in the presence of the protein were measured[57] as 1.1−1.2 s, and therefore the T_1 null ($0.693T_1$) is ∼0.80 s. To avoid misinterpretation of the data due to significant intensity losses due to T_1 relaxation, the binding epitopes were interpreted from the diffusion data acquired at $T = 600$ ms.

Transferred NOE as detected in NOESY experiments generally reaches a maximum within a few hundred milliseconds after which differential trNOE for individual ligand functionalities is equalized by spin diffusion of the NOE throughout the ligand proton spin system.[32,35,54] The distance dependence (r^{-6}) of the NOE theoretically limits its detection to nuclei that are within 5 Å of each other. However, when long mixing times are used, NOE may diffuse throughout a proton spin system, affecting remote nuclei not directly involved in dipolar coupling. Spin diffusion is especially effective in aliphatic chains such as caprylate and is less effective in molecules such as dansylglycine containing quaternary carbons or heteroatoms. Other ligand epitope mapping methods, such as saturation transfer difference (STD),[58−61] utilize very long experimental times for magnetization transfer (∼2 s). In the STD experiment, changes in ligand resonance intensity are monitored after selective irradiation of protein spins, which transfer magnetization to the spins of binding ligands.[59] Information about the binding specificity can be lost due to spin diffusion and T_1 relaxation when such long magnetization transfer times are used.[30] However, the experiment is a rapid, effective screening method that is a useful complement to the diffusion experiment described here, which provides more detailed epitope information at the expense of an increased experimental time.

Interpretation of Ligand Epitope Maps. The epitopes presented in Figure 4 provide a general picture of the dansylglycine and caprylate binding surfaces as the ligands interact with multiple albumin binding sites. However, the diffusion coefficients and hence epitopes are weighted toward the conformations at the primary binding site, drug site II, because the diffusion method is much less sensitive in detecting trNOE of weakly binding ligands.[29] In other ligand−protein systems where a single binding site exists, the ligand epitope revealed by the NMR diffusion results would purely reflect the ligand binding surface at that single specific site.

In the CAP−HSA solutions, the interactions of caprylate with HSA were so strong that the CAP *H2* and CAP *H4* resonances dipped below the baseline in the subtracted spectra (especially at the higher gradient amplitudes), leading to faster intensity decay and diffusion coefficients, as well as κ values that are not easily interpreted. Indeed, the structure of this molecule suggests that spin diffusion might act to equalize the NOE contributions to individual functional groups and yield a nonspecific epitope map. Although the κ values presented (Figure 4 and Table S1, Supporting Information) for caprylate suggest this may be a possibility, the CAP *H1* methylene group has slightly higher κ values in the solutions studied and is therefore most affected by trNOE (Figure 4A,B). The carboxyl group of fatty acids interacts electrostatically with Arg410 in HSA's drug binding site II,[3,5] and the CAP *H1* methylene group affected most by trNOE in the diffusion results is adjacent to the carboxyl group. Therefore, the diffusion results yield a reasonable epitope given the known interactions of fatty acids with HSA.

Based on the epitope map for 25:1 DG:HSA, the primary interaction of dansylglycine with HSA is similar to caprylate's (Figure 4C). The glycine methylene group (DG *H6*) shows the strongest interaction with HSA and may compete with caprylate for the Arg410 cationic side chain at this primary binding site for both ligands. The *N*-methyl groups (DG *H7*) show the second strongest interaction with the protein. As the aromatic rings interact hydrophobically with Tyr411 on HSA, the *N*-methyl groups may project away from the plane of its ring to interact strongly with other protein amino acid side chains in the binding pocket.

Ternary Complex Formation. Although the binding of many HSA drug site II and caprylate[46,47,55,62] have been well-characterized individually, less is known about the simultaneous interactions of multiple ligands with this protein. Standard binding assays with fluorescence or radioactive detection schemes, while sensitive, fail to reveal information about simultaneous complexation of multiple ligands due to the use of unlabeled ligand in a competitive assay format. The results discussed below show that simultaneous complexation of multiple ligands is revealed

(55) Ashbrook, J. D.; Spector, A. A.; Fletcher, J. E. *J. Biol. Chem.* **1972**, *247*, 7038−7042.
(56) Ravindranathan, S.; Mallet, J.-M.; Sinay, P.; Bodenhausen, G. *J. Magn. Reson.* **2003**, *163*, 199−207.
(57) Vold, R. L.; Waugh, J. S.; Klein, M. P.; Phelps, D. E. *J. Chem. Phys.* **1968**, *48*, 3831−3832.
(58) Mayer, M.; Meyer, B. *Angew. Chem., Int. Ed.* **1999**, *38*, 1784−1788.
(59) Mayer, M.; Meyer, B. *J. Am. Chem. Soc.* **2001**, *123*, 6108−6117.
(60) Möller, H.; Serttas, N.; Paulsen, H.; Burchell, J. M.; Taylor-Papadimitriou, J.; Meyer, B. *Eur. J. Biochem.* **2002**, *269*, 1444−1455.
(61) Murata, T.; Hemmi, H.; Nakajima, M.; Yoshida, M.; Yamaguchi, I. *Biochem. Biophys. Res. Commun.* **2003**, *307*, 498−502.
(62) Chignell, C. F. *Mol. Pharmacol.* **1969**, *5*, 244−252.

by simple diffusion-based NMR methods that do not require special spectroscopic labels for either the protein or the ligands.

As shown in epitopes A and B in Figure 4, the relative order of the epitope values for caprylate is the same whether or not dansylglycine is present, pointing to one dominant binding orientation. However, with the exception of DG *H2*, the epitope values for the aromatic ring protons depend on the presence and amount of caprylate (Figure 4C−E). This suggests that when the caprylate is added, the initial orientation of dansylglycine is less favored energetically and the ligand may reorient to adopt a more stable conformation. Additionally, the conformation of the protein binding pocket may change to accommodate caprylate binding, resulting in slightly different contacts to the dansylglycine aromatic protons. Although the individual contributions of ligand and protein conformational changes cannot be resolved in these experiments, deuterating the protein would render the protein contribution indetectable. The epitopes show the same significant interactions of the DG *H6* methylene group and the DG *H7 N*-methyl groups with the protein in the presence or absence of caprylate.

Figure 4 shows that the relative κ values for the different dansylglcyine and caprylate functional groups increase and become more similar when the second ligand is added. Furthermore, increased curvature in the diffusion plots is observed for *all* ligand protons. Similarity of the κ values suggests that spin diffusion may be a factor in the analysis of these epitopes, as also suggested by the appearance of cross-peaks from many of the DG aromatic protons to DG *H6* in Figure 5. However, the κ values measured are unique for the different dansylglycine protons, suggesting that the curvature is arising from trNOE and not solely spin diffusion or chemical exchange. Additional studies with deuterated ligands would provide insight into the individual contributions of spin diffusion and trNOE to the measured κ values.

The NOESY spectrum presented in Figure 5 for the 25:25:1 DG:CAP:HSA solution reveals the simultaneous binding of both ligands to HSA, evidenced by negative intraligand cross-peaks. As the HSA binding pockets can accommodate both ligands in solutions containing dansylglycine and caprylate, each ligand may be held more tightly in those binding pockets than when the competing ligand is not present. The higher absolute κ value for CAP *H1* compared to DG *H6* in the 25:25:1 solution suggests that the CAP *H1* group is closer to the protein than the DG *H6* group. This result is not surprising since caprylate, due to its size and flexibility, probably packs into the HSA binding pockets more tightly than the bulkier, more rigid dansylglycine. The difference in absolute κ values could also result from the difference in overall binding stoichiometry of the two ligands.

It is also possible that both ligands fit into a single pocket due to allosteric mechanisms that increase local motions of the protein at a common binding site, e.g., drug site II.[63,64] Figure 3 shows that the most curved diffusion data are observed for the 25:25:1 solution. Enhanced curvature in NMR diffusion results measured for competing ligands, something not previously observed in the literature, suggests that, in addition to protein conformational changes that may alter ligand−protein contacts, some trNOE actually comes from the second ligand. The negative ilNOE (boxed cross-peaks in Figure 5)[38−41] observed between dansylglycine and caprylate confirms NOE transfer between the two ligands at common HSA binding sites. Cross-peaks between the two ligands were not observed in a control spectrum acquired for a solution containing the ligands only (Figure S2, Supporting Information).

Like trNOE, detection of ilNOE (also referred to as ILOE in the literature)[38−41] cross-peaks is distance-dependent (r^{-6}); as such, the phenomenon is only measured for ligands in very close proximity in common protein binding pockets. Molecular modeling studies revealed the thermodynamic feasibility of simultaneous binding of DG and medium chain length fatty acids in HSA drug binding site II (table of contents graphic).[65] Thus it is likely that ilNOE contributes to the increased absolute and relative κ values obtained from the diffusion data for both dansylglycine and caprylate when the other ligand is present.

It is possible that the ilNOE cross-peaks could be protein-mediated; i.e., the NOE is transferred from one ligand to the next via the protein protons. However, in other systems it has been determined that protein-mediated effects are dependent on ligand geometry.[38,66] The contributions of protein-mediated NOE to ilNOE observed by the diffusion NMR method will be more easily determined in future studies of ligand−protein systems with a 1:1 binding stoichiometry, since the diffusion-based epitopes will represent the ligand geometry at a single binding site.

Conclusions

This is the first known report of ilNOE detected by diffusion measurements and shows the potential of diffusion NMR spectroscopy for characterizing other ternary protein structures such as enzyme−substrate interactions requiring a cofactor for catalysis, as well as drug−albumin interactions where bioavailability may be influenced by binding of endogenous ligands in vivo.[44] As demonstrated with the dansylglycine−caprylate−HSA system, determination and analysis of ligand binding epitopes by diffusion NMR spectroscopy have provided unique insight into the simultaneous interactions of HSA with these two ligands. Information about these interactions would be difficult to determine by other methods, since only dansylglycine is fluorescent and no crystal structure has been obtained for HSA with either or both ligands. Because ilNOE is strongest for ^{1}H−^{1}H interactions, ternary complex formation is readily detected by the universal NMR detector, precluding the need for specially labeled ligand or protein. However, the use of labeled compounds would facilitate a more quantitative investigation of the contribution of ilNOE, spin diffusion, and protein conformational changes to the curvature measured in the diffusion data.

Like trNOE, ilNOE is detected at longer diffusion times and is not obvious from a simple numerical evaluation of diffusion coefficients. Detection of ilNOE using NMR diffusion measurements is a rapid and simple alternative to 2D experiments, because the epitopes are determined from a single diffusion data set rather than a series of lengthy experiments. The results from the diffusion experiment are also of higher digital resolution and relatively easy to interpret, in contrast to 2D NOE methods

(63) Oida, T. *J. Biochem.* **1986**, *100*, 1533−1542.
(64) Birkett, D. J.; Myers, S. P.; Sudlow, G. *Mol. Pharmacol.* **1977**, *13*, 987−992.
(65) Lucas, L. H. University of Kansas: Lawrence, KS, 2004.
(66) Zheng, J.; Post, C. B. *J. Magn. Reson., Ser. B* **1993**, *101*, 262−270.

that are affected by T_1 relaxation and distance-restraint parameters used in determining bound ligand structures.[67]

The binding epitopes generated from the NMR diffusion data show that for both dansylglycine and caprylate, the methylene group adjacent to the carboxylate functionality interacts most strongly with HSA. This suggests a common electrostatic binding motif, although the two ligands are markedly different in size and shape. The changing epitopes observed for dansylglycine as caprylate is added and the NOESY cross-peaks observed for the protein solution containing both ligands point to the conformational adaptability of HSA, showing that this protein's flexible binding pockets can accommodate multiple ligands. Collectively, these results shed light on the conformational dynamics of a protein with affinity for a variety of ligands.

Although drug and inhibitor molecules are usually designed with specificity for a single binding site on a target protein or enzyme, characterizing interactions of such small molecules with nontarget proteins such as HSA is important in drug development. The NMR diffusion method is useful for the quantitative analysis of ligand binding epitopes with both target and nontarget proteins and thus aids in the understanding of structure−activity relationships affecting drug efficacy. In addition, this approach allows the investigation of competitive binding interactions involving endogenous ligands. The results presented show that NMR diffusion and NOE experiments provide useful information regarding protein−ligand and ligand−ligand interactions that might be encountered in vivo. This information is needed when characterizing drug bioavailability and could also aid in developing potent enzyme inhibitors by an optimize-and-link synthetic strategy.

Acknowledgment. L.H.L. acknowledges the support of the NIH Training Grant in the Dynamic Aspects of Chemical Biology (2 T32 GM08545) and thanks the ACS Division of Analytical Chemistry for a graduate fellowship sponsored by Eli Lilly. Que Van generously provided the WET pulse sequence used for solvent suppression.

Supporting Information Available: Experimental details regarding gradient calibration, acquisition, and processing parameters for the NMR data and viscosity measurements, diffusion data for the 25:1:1 DG:CAP:HSA solution illustrating chemical exchange effects, NOESY spectrum of the dansylglycine−caprylate mixture without HSA, and a table of ligand diffusion coefficients and κ values for the diffusion experiments performed at $T = 600$ ms. This material is available free of charge via the Internet at http://pubs.acs.org.

JA0479538

(67) Eisenmesser, E. Z.; Zabell, A. P. R.; Post, C. B. *J. Biomol. NMR* **2000**, *17*, 17−32.